An Analytic Approach Describing Structural Effects on the Properties of Molecular Fluids

R. LeSar*

Theoretical Division, Los Alamos National Laboratory, Los Alamos, New Mexico 87545

Received: October 9, 2000; In Final Form: February 14, 2001

An analytic approach is used to evaluate how the angular structure of a molecular fluid contributes to its thermodynamic properties. The average interactions (energy, forces, etc.) between molecules are first expressed as integrals over a spherical-harmonic expansion of the pair distribution function of the fluid. Angularly averaged interactions for systems described by site−site representations of the intermolecular potentials are then developed. Specifically, homonuclear diatomic molecules described by two-site potential are considered in this paper. These results are used to examine the role that fluid structure plays in determining the average energy, pressure, and forces on a molecule, using as comparison simulation data on dense, fluid nitrogen.

I. Introduction

How the thermodynamic properties of a molecular fluid depend on the structure of that fluid has long been of interest.[1] Much work has been done to develop descriptions of the fluid based on a variety of order parameters describing the local correlations between molecular orientations and positions. Most applications of those descriptions have yielded information about the structure of the fluid. Here, we wish to take those descriptions a step further and use them to show how the details of the structure contribute to the bulk properties of the fluid.

We shall express the average interactions (energy, forces, etc.) between molecules in the fluid as integrals over the pair distribution function.[1] By writing the pair distribution function as an expansion in the spherical harmonics, the average interactions can then be expressed as sums of integrals of the expansion coefficients of the distribution function ($g_{l_1l_2m}$) times quantities that are integrals of the interaction functions times the spherical harmonics. Since the $g_{l_1l_2m}$ contain all the information about the structure of the fluid, while the other terms depend only on the form on the interatomic potential, we can examine how the structure contributes to the average interactions. For comparison, we shall refer to computer simulations, with essentially the same intermolecular potential, in which the various expansion parameters were calculated. Specifically, we shall use the results from a Monte Carlo simulation of fluid nitrogen published some years ago by Belak et al.[2]

In addition to thermodynamic quantities, we shall also compare to simulation results for the change in the N_2 intramolecular vibrational frequency. The shifts in frequency of the intramolecular vibrations provide a direct measure of the forces acting on the molecules, and so there has been experimental and theoretical interest in determining these quantities. For example, with the use of diamond-anvil cells, frequency-shift measurements have been extended into the 100 GPa range[3] as well as to temperatures greater than 1000 K.[4,5] Coupled with shock-wave experiments,[4,5] these advances provide frequency-shift data over a huge range of density and temperature, providing a unique test for models of forces between molecules in fluids. In addition to the experimental studies, there have been a number of theoretical treatments of the shift in the intramolecular vibrational frequencies in dense fluids.[6−10] Many of these studies involve the use of a mean-field description of the forces acting on the molecules that arises from an early model of Schweizer and Chandler,[6] who approximated the fluid with a hard-sphere model. This latter approach is thus based on a highly approximate view of the structure of a molecular fluid. To assess and improve that and other models, more information is needed about how the structure of a fluid contributes to the forces acting on the molecules. Here we present a way to extract that information.

In section II, we show how to represent the angularly averaged interactions for systems described by a site−site intermolecular potential. Specifically, we treat homonuclear diatomic molecules described by 2-site potentials, though the procedure is easily generalized. In section III, we use these results to examine the role that fluid structure plays in determining the average energy, pressure, and forces on a molecule, based on results from Monte Carlo simulations of Belak et al.[2] We focus on the computer simulated $g_{l_1l_2m}$ because we can compare the analytical results with average values for the thermodynamic quantities from the simulations to evaluate the convergence of the expansions. An alternative approach would be to combine the expressions given below with analytic forms of the $g_{l_1l_2m}$ that have been derived by Steele and Sandler[11] and Patey and co-workers[12] some years ago. This latter approach would yield a completely analytic theory for both the structure and thermodynamics of molecular fluids. The goal of the present work, however, is to show how well the analytical forms converge to known values as well as to show how the structure of the fluid affects the thermodynamic properties. Comparison with accurate computer simulations is more appropriate for that purpose.

II. Theory

A. Analytical Results. The average value of any quantity that depends on the relative positions and orientations of linear molecules in a fluid can be written as an integral over the pair distribution function. For example, the average potential energy per molecule of a system described by a sum of pair potentials (of the form $U = \sum_{l>k} V(R_{kl}, \Omega_k, \Omega_l)$) can be written as[1]

* E-mail: lesar@lanl.gov. Fax: 505-665-3909.

10.1021/jp0036994 CCC: $20.00
Published on Web 08/28/2001

$$\langle U\rangle = \frac{1}{2}\frac{\rho}{(4\pi)^2}\int V(\mathbf{R},\Omega_1,\Omega_2)g(\mathbf{R},\Omega_1,\Omega_2)\,d\mathbf{R}\,d\Omega_1\,d\Omega_2 \quad (1)$$

where ρ is the density, $\mathbf{R}$ is the vector connecting the centers of mass of the molecules, and $\Omega_{1(2)}$ are the angles (θ,ϕ) between the molecular orientations and $\mathbf{R}$. The pair distribution function $g(\mathbf{R},\Omega_1,\Omega_2)$ can in turn be expressed as an expansion over the spherical harmonics Y_{lm} as[1]

$$g(\mathbf{R},\Omega_1,\Omega_2) = 4\pi\sum_{l_1,l_2,m} g_{l_1l_2m}(R)Y_{l_1m}(\Omega_1)Y_{l_2\bar{m}}(\Omega_2) \quad (2)$$

where R is the magnitude of $\mathbf{R}$. We thus can write

$$\langle U\rangle = 4\pi\rho\sum_{l_1,l_2,m}\int g_{l_1l_2m}(R)U_{l_1l_2m}(R)R^2\,dR \quad (3)$$

where

$$U_{l_1l_2m}(R) \equiv \frac{1}{4\pi}\int V(\mathbf{R},\Omega_1,\Omega_2)Y_{l_1m}(\Omega_1)Y_{l_2\bar{m}}(\Omega_2)\,d\Omega_1\,d\Omega_2 \quad (4)$$

From eq 3, we see that all dependence of the energy on the fluid properties arises from the correlation functions $g_{l_1l_2m}(R)$. The potential energy enters only in the $U_{l_1l_2m}(R)$ terms, which need to be determined only once for a given potential.

If we had the correlation functions, $g_{l_1l_2m}(R)$ (e.g., from simulations[2] or theory[11,12]), and the $U_{l_1l_2m}(R)$ functions (or equivalent terms for other quantities), we could use eq 3 to examine how the structure of a fluid contributes to the average interaction energies, pressures, etc. We present in this paper an analytical method for evaluating these (l_1l_2m)-expansion coefficients to arbitrary accuracy. While the procedure used here is quite general, we apply it to a particularly simple case, that of homonuclear diatomic molecules described by a two-site intermolecular potential. We describe the derivational procedure in detail for the potential energy; other derivations are similar and are outlined in the Appendices. Previous work has evaluated similar expressions for the potential energy in terms of hypergeometric functions,[13] but here we take an approach that is easily extendible to quantities other that the potential energy and to more complicated molecular systems and intermolecular potentials.

We assume that the interaction energy between two molecules 1 and 2 has the form

$$V_{12} = \sum_{i=1}^{2}\sum_{j=1}^{2} v(r_{ij}) \quad (5)$$

where i and j are the interaction sites on molecules 1 and 2, respectively, r_{ij} is the distance between sites on different molecules, and v is the site−site potential.

Consider $U_{l_1l_2m}(R)$ as defined in eq 4. It is not, in general, possible to directly integrate U over the spherical harmonics, even for the simple potential used here. We proceed by first expanding the site−site potential in powers of L around $L = 0$, where $L = b_e/2$ and b_e is the separation between the sites on the same molecule, i.e.,

$$v(r_{ij}) = v(R) + \sum_{n=1}^{\infty}\left(\frac{\partial^n v}{\partial L^n}\right)_{L=0}\frac{L^n}{n!} = v(R) + \sum_{n=1}^{\infty}L^n\sum_{k=0}^{[n/2]}\frac{(\alpha_{ij}+\beta_{ij})^{n-2k}(1+\delta_{ij})^k}{k!(n-2k)!}V^{(n-k)} \quad (6)$$

where $V^{(n)}$ is defined as

$$V^{(n)} \equiv \left[\frac{1}{R}\frac{\partial}{\partial R}\right]^n v(R) \quad (7)$$

$$\alpha_{ij} = (-1)^{j+1}\,\alpha = (-1)^{j+1}\,R\cos(\theta_2)$$

$$\beta_{ij} = (-1)^i\beta = (-1)^i\,R\cos(\theta_1)$$

$$\delta_{ij} = (-1)^{i+j+1}\,\delta = (-1)^{i+j+1}\hat{n}_1\cdot\hat{n}_2 \quad (8)$$

Here, θ_1, θ_2, and $\phi_{12} = \phi_2 - \phi_1$ are the angles of the molecular bonds relative to the vector connecting the centers of mass,[1] and we take site 1 to be in the positive direction along the bond. For example, $V^{(2)} = (1/R)\partial/\partial R[(1/R)\partial v(R)/\partial R]$. In eq 6, $[n/2] = n/2$ for n even and $(n-1)/2$ for n odd. To evaluate $U_{l_1l_2m}(R)$, we sum $v(r_{ij})$ in eq 6 over the sites ij, multiply by the spherical harmonics, and integrate over angles. We find

$$\tilde{U}_{l_1l_2m}(R) \equiv \frac{U_{l_1l_2m}(R)}{4\pi N_{l_1m}N_{l_2\bar{m}}} = 4v(R)\delta_{l_1,0}\delta_{l_2,0} + 4\sum_{n=1}^{\infty}L^{2n}\sum_{k=0}^{n}R^{2n-2k}V^{(2n-k)}S_{2n,k}^{0,0,0}[l_1l_2m] \quad (9)$$

where δ_{ij} is 1 if $i = j$ and 0 otherwise and the functions $S_{n,k}^{w,y,z}[l_1l_2m]$ are given in Appendix A. The factors N_{lm} are the normalization constants for the spherical harmonics, which are defined elsewhere.[10] The result given in eq 9 is valid for any form of potential, given an evaluation of $V^{(n)}$. We give here results for the two most commonly used forms used to describe intermolecular potentials: (1) $v = 1/r_{ij}^M$ and (2) $v = \exp[-\alpha r_{ij}]$.

For a site−site potential of the form $v = 1/r_{ij}^M$, we have

$$V^{(n)} = (-1)^n\frac{(M+2[n-1])!!}{(M-2)!!}R^{-(M+2n)} \quad (10)$$

where !! indicates the double factorial. Inserting this expression in eq 9 yields a computationally simple way to evaluate all possible $U_{l_1l_2m}(R)$. We can also generate analytical expressions for each term in the series. For example, U_{000} $(= \tilde{U}_{000}$, the spherically averaged potential), is given by

$$U_{000}(R) = \frac{8}{R^M(M-2)!}J_0(M,x) \quad (11)$$

where $x = b_e/R$, $b_e = 2L$, and

$$J_0(M,x) = \sum_{k=0}^{\infty}\frac{(M+2k-2)!}{(2k+2)!}x^{2k} = \frac{(M-4)!}{2x^2}\left\{\frac{1}{(1+x)^{M-3}} + \frac{1}{(1-x)^{M-3}} - 2\right\} \quad (12)$$

The general function is

$$J_n(M,x) = \sum_{k=0}^{\infty}\frac{(M+2k-2)!}{(2k+2)!}k^n x^{2k} \quad (13)$$

which has the recursion relation

$$J_{n+1}(M,x) = \frac{x\partial J_n}{2\,\partial x} \quad (14)$$

From eqs 14 and 12, all other values of J_n can be derived. Note

that $U_{000}(R)$ is finite for all $x > 1$, i.e., $R > b_e$, but diverges at $x = 1$. Equation 11 is equivalent to, but in a somewhat different form than, expressions given elsewhere for the spherically averaged $1/R^M$ site−site potential.[13]

A strength of the current procedure is that it is easily extendable to other forms of potentials. For example, for an exponential site−site potential, $v = \exp[-\alpha r_{ij}]$, we have ($n > 0$)

$$V^{(n)} = (-1)^n \frac{\alpha e^{-\alpha R}}{R^{2n-1}} \left[\sum_{t=0}^{n-1} \frac{1}{2^t t!} \frac{(n-1+t)!}{(n-1-t)!} (\alpha R)^{n-1-t} \right] \quad (15)$$

Equations 9 and 15 can be used either to numerically evaluate $U_{l_1 l_2 m}(R)$ or to generate analytical expressions for the different terms in the series over n. Doing the latter for $U_{000}(R)$, we find (with $x = \alpha b_e$)

$$U_{000}(R) = \frac{8 e^{-\alpha R}}{\alpha} \left\{ \alpha K_0(x) - \frac{2}{R} K_1(x) \right\} \quad (16)$$

where

$$K_0(x) = \sum_{k=0}^{\infty} \frac{x^{2k}}{(2k+2)!} = \frac{\cosh(x) - 1}{x^2} \quad (17)$$

$K_0(x)$ is the first term in the general series of functions

$$K_n(x) = \sum_{k=0}^{\infty} \frac{k^n x^{2k}}{(2k+2)!} \quad (18)$$

All $K_n(x)$ with $n > 0$ can be evaluated from eq 17 and

$$K_{n+1}(x) = \frac{x}{2} \frac{\partial K_n}{\partial x} \quad (19)$$

Expressions similar to eq 3 can be derived for other thermodynamic quantities. In each case, we need expressions for the expansion coefficients. For example, the expressions for the pressure, $P_{l_1 l_2 m}(R)$, are given in Appendix C. In Appendix D, we introduce the generalized derivative $F^{(n)} = (\partial^n v / \partial b^n)_{b_e}$, where the force along the bond of a molecule due to the rest of the molecules is $f \equiv F^{(1)}$ and the curvature due to that interaction is $k \equiv F^{(2)}$, and give expressions for the coefficients in a spherical harmonic expansion of these quantities.

B. Tail Corrections. It is standard in molecular dynamics or Monte Carlo simulations of molecular fluids to cut off the interactions between molecules at some distance. A *tail correction* is then added[14] to approximate the contribution to the energy from molecules beyond the cutoff. The tail correction is usually found by assuming $g_{000} = 1$ and all other $g_{l_1 l_2 m}(R) = 0$ for distances beyond the cut off. Since the cutoff distance R_c is large, only the long-range part of the site−site potential, which is usually of the form $-C/R^6$, is included. Using eqs 11 and 12, we find that the tail correction for the potential energy (when using a two-site potential) is

$$U_{\text{tail}} = -\frac{2\pi\rho C}{3R_c^3} \sum_{k=0}^{\infty} (2k+4) x_c^{2k} \quad (20)$$

where $x_c = b_e/R_c$. The tail correction for the pressure (Appendix C) is given by

$$P_{\text{tail}} = -\frac{2\pi\rho^2 C}{9R_c^3} \sum_{k=0}^{\infty} (2k+4)(2k+6) x_c^{2k} \quad (21)$$

Similar expressions are easily derivable for the force and force constant (Appendix D). Note that in most simulations with potentials of this kind, the tail corrections have been approximated with just the first terms in eqs 20 and 21, respectively.

C. Comparison with Simulations. We can now use the expressions given above to examine how different terms in the expansion over the spherical harmonics, and thus different aspects of the fluid structure, contribute to the thermodynamic properties of a molecular fluid. We compare our results to simulation data, rather than using analytic forms for $g_{l_1 l_2 m}(R)$, because we are interested in the convergence properties of the expansions and want to compare with known results. We base our results on simulation data for dense fluid N_2, for which thermodynamic data, intramolecular vibrational frequency shifts, and radial distribution functions are available from Monte Carlo simulations by Belak et al.[2] The intermolecular potential used in their simulations was from Etters et al.[15] and employed an exponential-six site−site potential with two sites per molecule (separated by a distance b_e) and an electrostatic term that summed the interactions of charges distributed along the bond. The electrostatic interactions are relatively unimportant in high-density fluids, so we do not include them here. An additional approximation arises because of the form used for the short-range part of the Etters site−site potential.[15] That potential was divided into three regions: for $r_{ij} < 3.01$ Å, an exponential potential of the form $A \exp[-\alpha r_{ij}]$ was used; for $r_{ij} > 3.45$ Å, they used an exponential potential with different parameters; and for 3.01 Å $\le r_{ij} \le$ 3.45 Å, a spline interpolation between the two. The long-range part of the potential is given as $-C/r_{ij}^6$. We cannot apply the equations outlined in section II to this form of short-range potential by simply switching from one form of $V^{(n)}$ to another at the appropriate distances, because at each intermolecular separation a number of intersite distances contribute to the energy, pressure, etc. in the integrals over angles. Since we are primarily interested in comparing to dense fluid results, where small separations dominate, we used the potential for $r_{ij} < 3.01$ Å, which is of the form $v(r) = Ae^{-\alpha r} - C/r^6$, where $A = 1.4725 \times 10^7$ K, $C = 1.7913 \times 10^5$ K, and $\alpha = 3.4795$/Å. The separation between sites is $b_e = 1.094$ Å. Belak et al.[2] had an error in their tail corrections; they were equivalent to using three times the first term in the series in eq 20. We corrected their results in the comparisons made below.

We will compare to simulation results for the average potential energy $\langle U \rangle$, the average pressure $\langle P \rangle$ and the shifts in the intramolecular vibrational frequency $\langle \omega \rangle$. The procedure for determining the frequency shifts is given in Appendix E and is equivalent to what was done in the simulations.[2] To evaluate the different contributions for the average quantities, we used eq 3 for the energy (or the equivalent expressions for other quantities). We took the $g_{l_1 l_2 m}(R)$ values from the Monte Carlo simulations and then numerically integrated each term in the expansions over ($l_1 l_2 m$), checking for convergence in the sum over ($l_1 l_2 m$).

III. Results

A. Properties of $U_{l_1 l_2 m}(R)$, etc. The quantities $U_{l_1 l_2 m}(R)$, $P_{l_1 l_2 m}(R)$, etc. are expressed as infinite series (cf. eq 9 for U and the Appendices for the other quantities). Here we discuss the convergence properties of these sums, which determines how

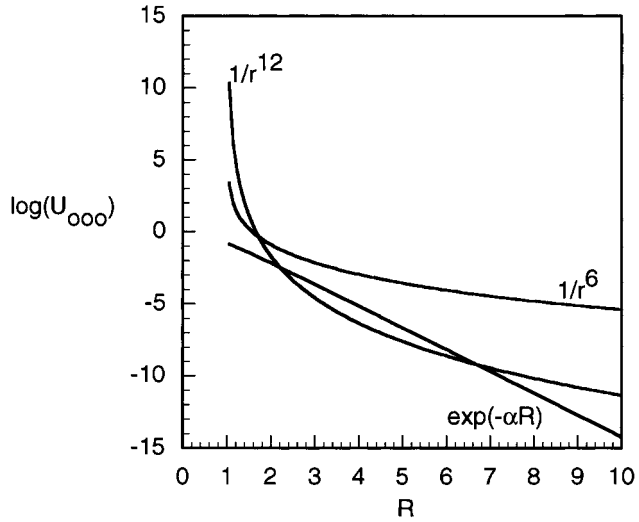

Figure 1. Spherically averaged potentials $U_{000}(R)$ for $1/R^6$, $1/R^{12}$, and $\exp(-\alpha R)$ site−site potentials. The separation between sites (b_e) is 1 and α is 3.5, approximately what is found for N_2.

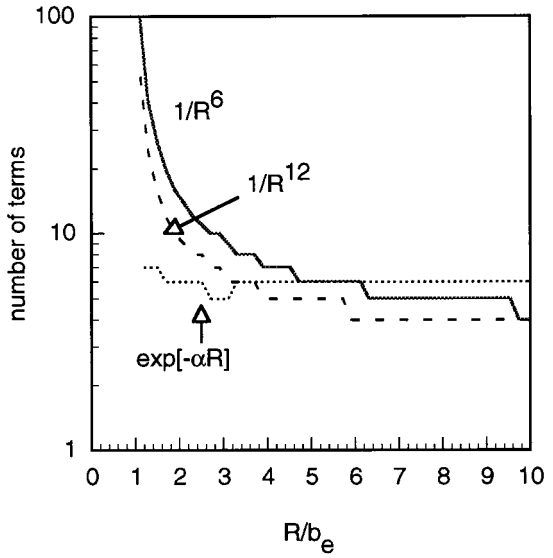

Figure 2. Number of terms needed in eq 16 to meet the convergence requirements defined in the text. The solid curve is for a $1/R^6$ potential, the dot−dash for a $1/R^{12}$ potential, and the dashed for a $\exp[-\alpha R]$ potential.

useful they can be. We note that the convergence properties of all the quantities studied here, independent of quantity and values of (l_1l_2m), are very similar to those for $U_{l_1l_2m}(R)$, which in turn are similar to those of $U_{000}(R)$. Thus, we can focus on the properties of $U_{000}(R)$, which are shown in Figure 1 for the site−site potentials considered here. The advantage to using $U_{000}(R)$ is that we have analytical series for both $1/R^M$ and $\exp[-\alpha R]$ potentials that have the same basic form (i.e., in powers of $x = b_e/R = 2L/R$) as the general expression in eq 9. We can also determine the accuracy of the final results by comparing to the exact analytical expressions given in eqs 11 and 16, respectively.

Based on the form of eqs 9 and 11, we define the quantity $S_n = \sum_{k=1}^{n} U_k$, where we note that the $k=0$ term is not included. We then sum eq 11 over k until $U_k/S_{k-1} < \zeta$, where ζ is a specified convergence parameter. With ζ set to 0.0001, we obtain the results shown in Figure 2 for $1/R^6$, $1/R^{12}$, and $\exp[-\alpha R]$ potentials, where we used parameters that roughly correspond to N_2 ($b_e = 1$ and $\alpha = 3.5$). In that figure, we plot the number of terms needed to meet the convergence criteria as a function of the distance measured in multiples of the length b_e. We see that for an $\exp[-\alpha R]$ potential, no more than six or seven terms are needed to calculate U_{000} to better than 1 part per 10^6 at any distance. However, for a $1/R^M$ potential, the convergence properties of U_{000} depend on distance. For large R, the number of terms needed for convergence is fairly small. As R/b_e approaches 1, however, the number of terms needed for convergence increases dramatically, a behavior which arises from the divergence of U_{000} when $R = b_e$ (cf., eq 11 and Figure 1). The closest approach in dense fluid nitrogen is roughly 2.5 Å, or $R/b_e \approx 2.1$. Even for a $1/R^{12}$ potential, only 14 terms are needed at that distance to reach the desired convergence. For most distances, no more than 5 or 6 terms are needed to obtain U_{000} to an accuracy better than 1 part in 10^6.[17]

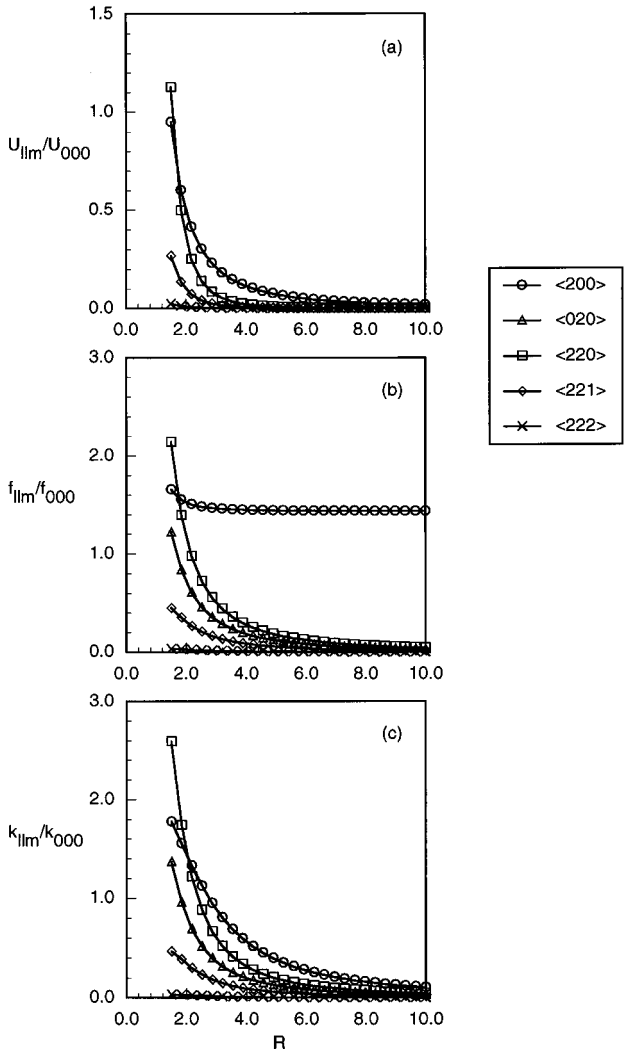

Figure 3. (l_1l_2m)-Expansion terms as fractions of the (000) term for a $1/R^6$ site−site potential. The symbols are: circles (200), squares (220), diamonds (221), and crosses (222). Additionally, (020) terms are given by triangles. (a) $U_{l_1l_2m}(R)$; (b) $f_{l_1l_2m}(R)$; (c) $k_{l_1l_2m}(R)$. The separation between sites is 1.

In Figure 3, we show values for $U_{l_1l_2m}(R)/U_{000}(R)$, $f_{l_1l_2m}(R)/f_{000}(R)$ (the force along the molecular bond) and $k_{l_1l_2m}(R)/k_{000}(R)$ (the force constant due to the intermolecular interactions) for the (l_1l_2m) values (200), (020), (221), and (222) for a $1/R^6$ potential. We do not show the $P_{l_1l_2m}(R)$, which are similar in form to $U_{l_1l_2m}(R)$. Similar plots are shown in Figure 4 for an $\exp[-\alpha R]$ potential. For both sets of plots, $b_e = 1$, while in Figure 4, α is 3.5 (similar to that used for N_2). Looking first at Figure 3a, we see that the (200) term, which is the same as the

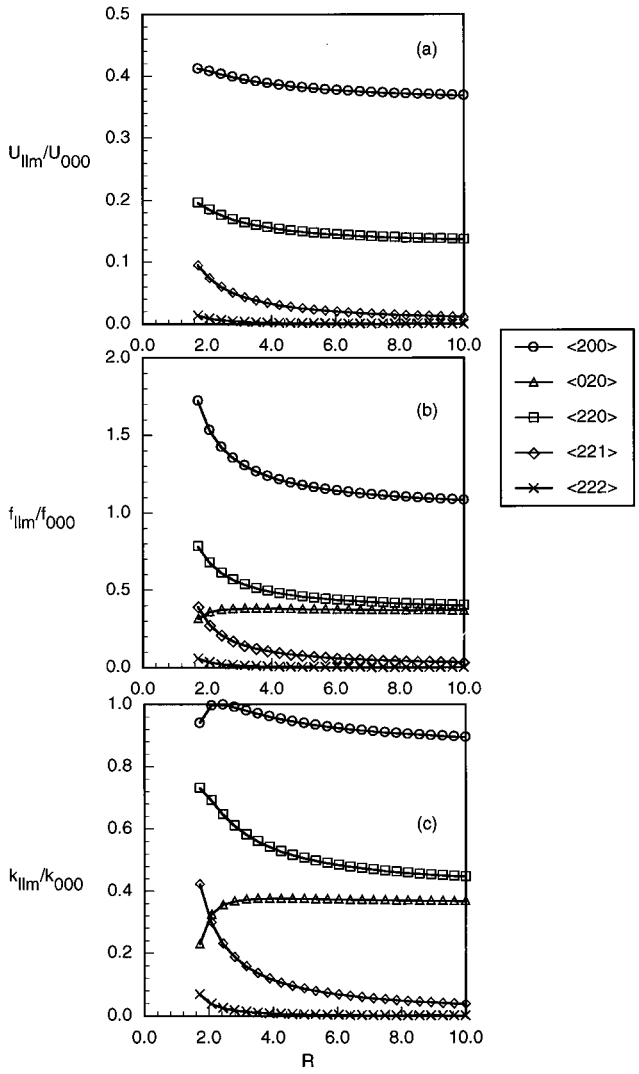

Figure 4. (l_1l_2m)-Expansion terms as fractions of the (000) term for a $\exp[-\alpha R]$ site−site potential. The symbols are the same as in Figure 3. The separation between sites is 1 and α is 3.5.

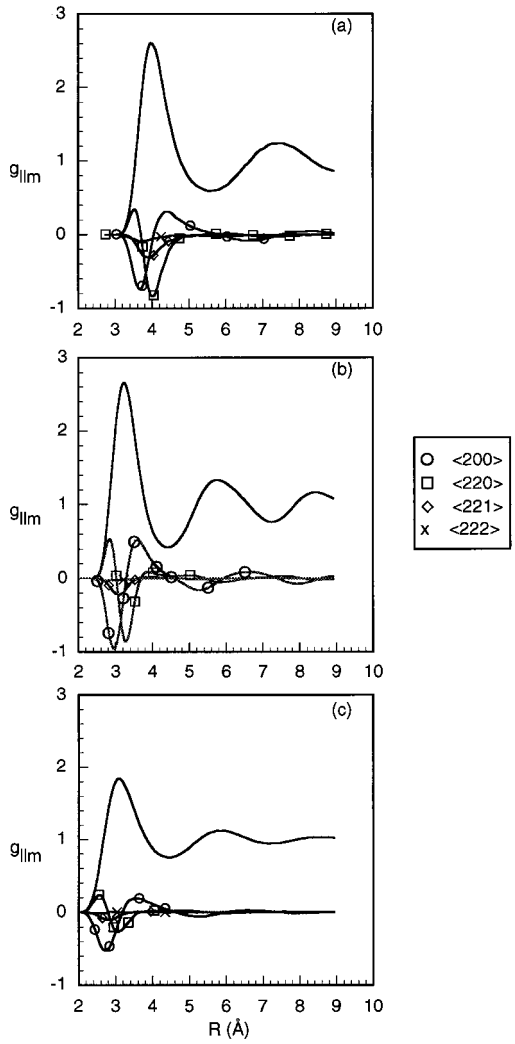

Figure 5. Expansion coefficients $g_{l_1l_2m}(R)$ for fluid N_2 from the simulations of Belak et al.[2] The solid curve is (000), the curve with circles is (200) (= (020) for homonuclear diatomics), with squares is (220), with diamonds is (221), and with X is (222). (a) normal liquid N_2 at zero pressure and 75 K; (b) fluid N_2 at 10 GPa and 600 K, (c) 15 GPa and 3000 K.

(020) term for both the potential and pressure, is the largest higher-order $U_{l_1l_2m}(R)$ for a $1/R^6$ potential, followed in order by the (220), (221), and (222) terms. Because f is defined as the derivative of the potential with respect to the bond length of molecule 1, the (200) and (020) terms for $f_{l_1l_2m}(R)$ are not equal, as shown in Figure 3b. The (200) term depends on the Legendre function P_{20}, which is largest when the molecule is pointed directly at its neighbor, and thus makes the largest contribution to the force along the bond. The behavior of $k_{l_1l_2m}(R)$ is roughly similar to that for $U_{l_1l_2m}(R)$.

Comparison of the $U_{l_1l_2m}(R)/U_{000}(R)$ in Figure 4a for an $\exp[-\alpha R]$ potential with that in Figure 3a for a $1/R^6$ potential shows somewhat different behavior. While the basic pattern is similar, with the (200) largest, followed by (220), (221), and (222), the magnitudes and R-dependence are quite different. All terms in the (l_1l_2m) expansion shown in Figure 3a go to zero faster than the $U_{000}(R)$ term at large R. However, for the exponential potential, the (200) term asymptotes to some finite multiple of $U_{000}(R)$, as does the (220) term. In 4b and 4c, we see that the R-dependences of $f_{l_1l_2m}(R)$ and $k_{l_1l_2m}(R)$ also differ greatly from their counterparts in 3b and 3c, respectively.

B. Application to Dense Molecular Systems. We can use the expressions derived here to examine how the structure of a fluid, as described by the correlation functions $g_{l_1l_2m}(R)$, contributes to the overall thermodynamic properties. As noted above, we will compare with the results of Belak,[2,16] who calculated $g_{l_1l_2m}(R)$ for a number of different pressures and temperatures for both solid and fluid N_2. We examine the convergence of the thermodynamic properties for three states: normal liquid N_2 ($P = 0$, $T = 75$ K, $\rho = 0.82$ g/cm^3); for a state near the melting line at high pressures ($P = 10$ GPa, $T = 600$ K, $\rho = 1.75$ g/cm^3); and for a state along the Hugoniot ($P = 15$ GPa, $T = 3000$ K, $\rho = 1.69$ g/cm^3). In Figure 5, we show $g_{l_1l_2m}(R)$ for these cases. Note that the basic structures of the fluids at each state point are similar. The spherically symmetric term, $g_{000}(R)$, measures the correlation between the centers of mass of the molecules, the first peak representing the nearest neighbor molecules in the fluid.

To understand the ordering of the molecules in the fluid, it is convenient to introduce a set of "standard" relative orientations of a pair of molecules: P ($\theta_1 = 90°$, $\theta_2 = 90°$, $\Delta\phi = 0°$); X ($\theta_1 = 90°$, $\theta_2 = 90°$, $\Delta\phi = 90°$); T1 ($\theta_1 = 0°$, $\theta_2 = 90°$, $\Delta\phi = 0°$); T2 ($\theta_1 = 90°$, $\theta_2 = 0°$, $\Delta\phi = 0°$); L ($\theta_1 = 0°$, $\theta_2 = 0°$, $\Delta\phi = 0°$). Typically, $g_{200}(R)$ starts off negative at small intermolecular separations, becoming positive at approximately the nearest-neighbor separation, while $g_{220}(R)$ is positive at small separations and then becomes negative at distances somewhat

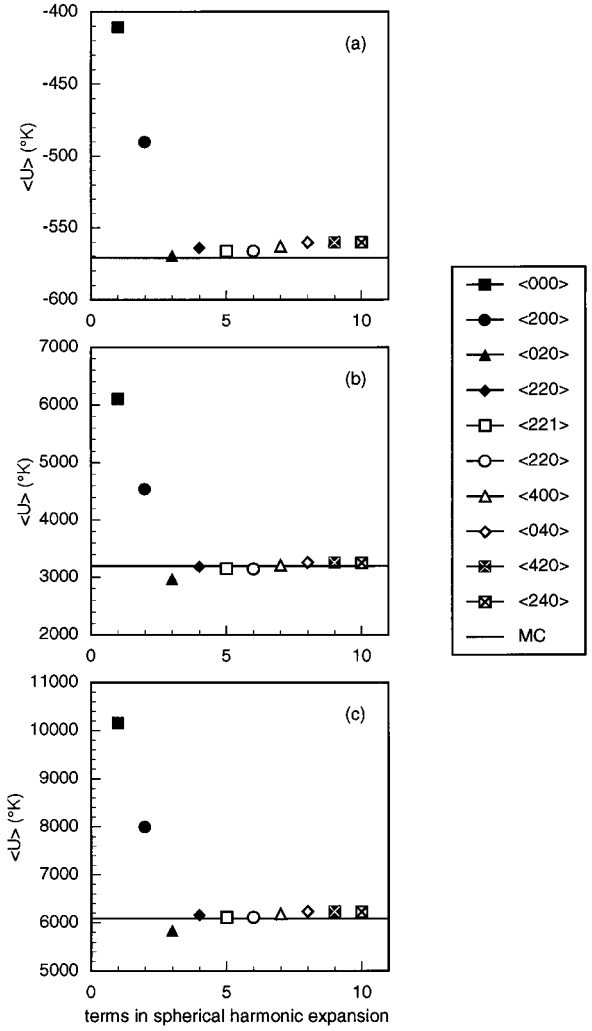

Figure 6. $\langle U \rangle$ as a function of the number of terms in its $(l_1 l_2 m)$ expansion. The symbols are defined in the figure and the horizontal solid line is from the Monte Carlo calculations. For (c), the result was determined from analytical fits described in reference 2. (a) $P = 0$ GPa and $T = 75$ K; (b) $P = 10$ GPa, $T = 600$ K; (c) $P = 15$ GPa, $T = 3000$ K.

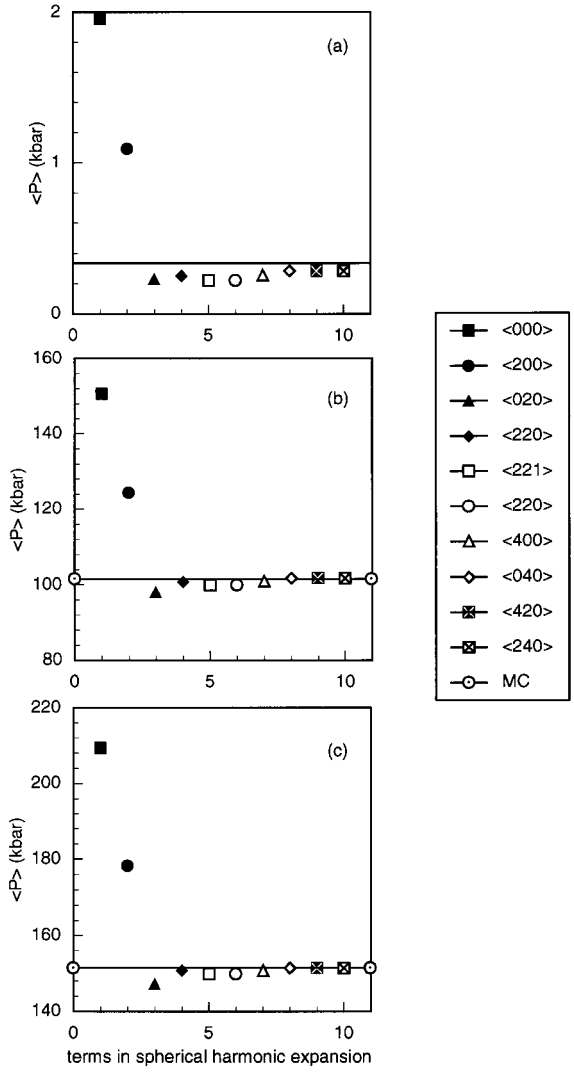

Figure 7. $\langle P \rangle$ as a function of the number of terms in its $(l_1 l_2 m)$ expansion. The symbols are defined in the figure and the horizontal solid line is from the Monte Carlo calculations.[2] (a) $P = 0$ GPa and $T = 75$ K; (b) $P = 10$ GPa, $T = 600$ K; (c) $P = 15$ GPa, $T = 3000$ K.

inside the first peak in $g_{000}(R)$. The shape of these two terms indicates that at small separations the molecules tend to align in X- and P-type configurations (with varying $\Delta\phi$),[16] while at distances approximately that of the nearest neighbors, T-type configurations begin to dominate. With the similarities in fluid structure, it will not be surprising that the contributions of the various terms in the $(l_1 l_2 m)$ expansion to the thermodynamics and the intramolecular vibrational frequency shifts will be qualitatively similar for all three state points.

In Figure 6 we show the convergence of the average potential energy $\langle U \rangle$ as a function of the number of terms in the $(l_1 l_2 m)$ expansion given in eq 3. The basic shape of the plots is essentially independent of density and temperature; the (000) term by itself is much too positive, but convergence is essentially reached when the (200) and (020) terms (which are equal for the potential energy) are included. As would be expected, the higher-order terms make more of a contribution for the denser material, but the expansion converges to a reasonably accurate result very quickly. For normal liquid N_2, the (000) term by itself is in error by about 25%, but when the (200) and (020) terms are included, the error drops to about 1.5% relative to the asymptotic value. The deviation between the value calculated in the Monte Carlo simulation and the present result is largely due to the somewhat different potential used in these calculations. The largest contribution to the error probably arises from neglecting the electrostatic contribution to the energy. For the $P = 10$ GPa and $T = 600$ K case, the (000) term by itself is too high by about 90%. Including (200) and (020) leads to a result that is too low by about 9%. The (220) term brings the result to within about 2%, but it is not until the (221), (222), (400), and (040) terms are included that the error drops below 1%. Under shock conditions ($P = 15$ GPa, $T = 3000$ K), the result with just (000) is 60% too high, with (200) and (020) about 10% too low. We need to include up to the (400) and (040) terms to drop the error to better than 1% relative to the MC result.

The convergence of the series over the $(l_1 l_2 m)$ to calculate the pressure (Appendix C) is shown in Figure 7, and the results largely parallel those for the energy. Once again, the deviations in the final result from the MC calculations are most likely due to the somewhat different potential used here than in the simulations. The relative contributions to the pressure from the various terms are similar to that for the potential energy: the (000) term alone is 600%, 50%, and 38% too high for the normal liquid, $P = 10$ GPa and $T = 600$ K, and $P = 15$ GPa and $T = 3000$ K states. Including the (200) and (020) terms reduces that

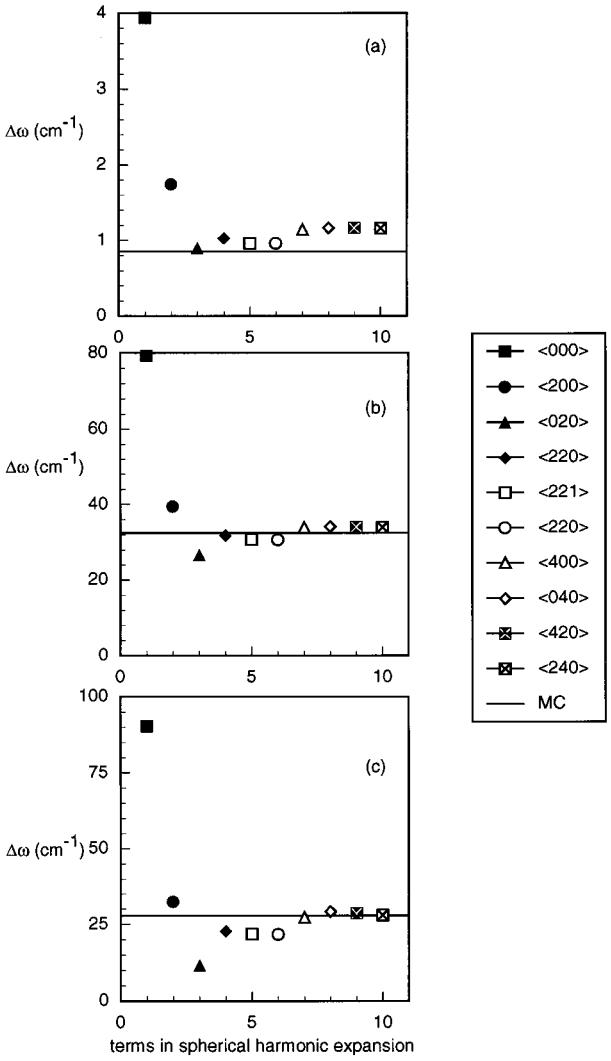

Figure 8. $\Delta\omega$ as a function of the number of terms in its (l_1l_2m) expansion. The symbols are defined in the figure and the horizontal solid line is from the Monte Carlo calculations. For (a) and (c), these results were determined from analytical fits described in ref 2. (a) $P =$ 0 GPa and $T = 75$ K; (b) $P = 10$ GPa, $T = 600$ K; (c) $P = 15$ GPa, $T = 3000$ K.

error to 17%, 3.6%, and 2.8%, respectively, relative to the converged result. Note that the large percentage errors for the normal liquid are somewhat misleading due to the small asymptotic value.

Rather than describe the contributions to the force and force constant separately, we consider here the change in intramolecular vibration frequency, which, as shown in Appendix E, depends on both *f* and *k*. As seen in Figure 8, while the detailed shape is somewhat different from that for $\langle U\rangle$ and $\langle P\rangle$, the general trend is the same; the (000) component greatly overestimates the average frequency change, but the series converges to the proper value. Using only the spherically symmetric term yields even greater error for the frequency than the energy or pressure, however, with a very large overestimation of the frequency shift. The result does not converge well to its final result until the (400) and (040) terms are included.

IV. Discussion

From Figures 6−8 we can examine the dependence of thermodynamic properties on the fluid structure, at least for fluid nitrogen. In all cases, terms up to (400) and (040) must be included for a converged result to be obtained. The pattern for all quantities is similar: the (000) term alone greatly overestimates the average value. This should not be surprising as the (000) term includes all relative orientations weighed equally, including those that would place nearby molecules aligned toward each other, with consequent small intermolecular separations and large repulsive contributions. Note that the (000) term also includes the long-range contributions, since only $g_{000}(R)$ does not vanish at large *R*. Adding the (200) and (020) terms for the energy $\langle U\rangle$ and pressure $\langle P\rangle$ yields a reasonable approximation to the converged result. Note that since all $U_{l_1l_2m}(R)$ functions are positive (Figures 3 and 4), the sign of each term's contributions to $\langle U\rangle$ is determined by the sign of $g_{l_1l_2m}(R)$ in Figure 5. Since in calculating $\langle U\rangle$ the (200) and (020) terms are negative, the final value for $\langle U\rangle$ is determined largely by the negative regions of $g_{200}(R)$, i.e., the X- and P-type configurations at distances less than and approximately equal to the nearest neighbor distance.

While the overall pattern of the convergence is similar for the force along the bond, *f*, the force constant, *k*, and the frequency change, $\Delta\omega$, there are significant differences. Using the (000) contribution alone still overestimates the converged result. However, adding just the (200) term yields a reasonable approximation to the final value. This can be understood by examining the values for $f_{l_1l_2m}(R)$ and $k_{l_1l_2m}(R)$ in Figure 4, where we see that the (200) term dominates, while the (020) values are smaller than that for (220). While the (020) term is smaller, including it does yield an underestimate of the frequency shift in Figure 8. Thus, stopping at the (200) term might be a reasonable approximation, but, at least for fluid nitrogen, that good agreement is fortuitous.

The central issue in modeling vibrational frequency shifts in molecular fluids is to obtain an accurate representation of the forces acting on the molecules. One model, due to Schweizer and Chandler (SC),[6] approximates the repulsive interactions from the potential of mean force for a molecule (described as two interpenetrating, noninteracting, hard spheres) in a fluid of hard spheres. The SC model has been shown to work well in describing frequency shifts in many molecular fluids over a wide range of densities,[7−10] which is somewhat surprising given the crude a representation of the fluid structure on which it is based. Indeed, a spherical-harmonic expansion of the interactions in the SC model, such as that in eq 3, would include only terms of the form (000), (200), (400), ... The behavior of $\Delta\omega$ in Figure 8 may provide an indication of why the SC model yields reasonable results for frequency shifts, at least for fluid nitrogen. For all three state-points in Figure 8, truncating the expansion at the (000) and (200) terms gives reasonable approximations to the converged values. Thus, the good agreement in the SC model may be a result of an effective truncation at the right place.

Another approach that has been used successfully in the study of vibrational frequency shifts is a mean-field Monte Carlo (MC) method.[2] This approach builds in a realistic dependence on fluid properties, but requires relatively time-consuming computer simulations and gives little insight into the generic behavior of frequency shifts. The central purpose of this paper is to extract from the MC results details of how the fluid structure contributes to the forces in the system in the hope of providing guidance for assessing current models and creating new ones. We had the same goal a number of years ago, when we used an expression similar to eq 3 to find an analytical form for the average force (*f*) along the bond of a diatomic molecule in a dense molecular fluid.[10] We found an approximate result by truncating at the spherically symmetric (000) term and by using

a hard-sphere form for $g_{000}(R)$. The expansion coefficient $f_{000}(R)$ was found by expanding f to third order in powers of b/R and integrating over the angles term by term. The expression derived there was inaccurate for two reasons: we truncated the expansion in b/R too soon, as shown in Figure 3; and there are significant contributions from the higher (l_1l_2m) terms in the expansion in eq 3 as we see in Figure 8. Here we have corrected those problems.

V. Summary and Conclusion

We have presented a systematic approach to derive spherical-harmonic expansions of thermodynamic quantities in molecular fluids whose interactions are described by site−site potentials. By expanding the quantities of interest (energy, pressure, forces, etc.) in powers of the distances between sites on a molecule, expressions are generated for integrals of those quantities over the spherical harmonics. While we showed results for systems described by two-site potentials, the approach is extendable to other systems. Given those expressions, average thermodynamic quantities can be calculated by integrating over the coefficients in a spherical-harmonic expansion of the pair distribution function. Combining those expressions with theoretical forms of the $g_{l_1l_2m}$ derived some years ago[11,12] would lead to a completely analytical description of the structure and properties of molecular fluids.

We used the spherical-harmonic expansions to examine the dependence of average thermodynamic quantities on the structure of the fluid, using distribution functions calculated from simulations of dense, fluid nitrogen.[2,16] We found that the expansions converged quickly, with reasonable values obtained with just a few terms. We also examined the convergence of the spherical-harmonic expansion of shifts in the intramolecular vibrational frequency. In light of these results, we then discussed models for vibrational frequency shifts in molecular fluids.[6]

Acknowledgment. I would like to thank J. F. Belak for use of his computer simulation results and M. S. Shaw for many helpful discussions. R. Eykholt provided assistance in summing the series to arrive at the results in eqs 12 and 16. This work was performed under the auspices of the U.S. Department of Energy and was supported in part by the Division of Materials Sciences of the U.S. D. O. E. Office of Basic Energy Sciences.

Appendix A. $T^{w,y,z}_{n,k}$ and $S^{w,y,z}_{n,k}$

We need to evaluate the integral of

$$T^{w,y,z}_{n,k} \equiv \frac{1}{k!(n-2k)!}\sum_{i=1}^{2}\sum_{j=1}^{2}(\alpha_{ij}+\beta_{ij})^{n-2k}(1+\delta_{ij})^{k}\beta_{ij}^{w}\,\delta_{ij}^{y}\,\alpha_{ij}^{z} \tag{A1}$$

over the spherical harmonics. We first expand $(\alpha_{ij}+\beta_{ij})^{n-2k}$ and $(1+\delta_{ij})^{k}$ in binomial series. Then we simplify those expressions by using the relations in eq 8 and noting that

$$\sum_{i=1}^{2}\sum_{j=1}^{2}\alpha_{ij}^{m}\,\beta_{ij}^{n}\,\delta_{ij}^{p} = (-1)^{m+p}\,\alpha^{m}\beta^{n}\delta^{p}\sum_{i=1}^{2}(-1)^{i(n+p)}\sum_{j=1}^{2}(-1)^{j(m+p)}$$
$$= 4\alpha^{m}\beta^{n}\delta^{p}\,\Xi_{n+m}\Xi_{m+p}\Xi_{n+p} \tag{A2}$$

where we define a function, Ξ_m, which equals 1 if m is even and 0 if m is odd. Note that eq A2 would need to be modified if another form of site−site potential was used (e.g., more than two sites).

Multiplying eq A1 by the spherical harmonics[10] and integrating over angles, we have

$$T^{w,y,z}_{n,k}[l_1l_2m] = N_{l_1m}N_{l_2\bar{m}}\,4R^{n-2k+w+z}\Xi_{n+w+z}S^{w,y,z}_{n,k}[l_1l_2m] \tag{A3}$$

where

$$S^{w,y,z}_{n,k}[l_1l_2m] = \frac{1}{k!(n-2k)!}\sum_{q=0}^{n-2k}\binom{n-2k}{q}\sum_{p=0}^{k}\binom{k}{p}\times$$
$$\sum_{s=0}^{p+y}\binom{p+y}{s}A^{q+w+s,p+y-s}_{l_1m}\,A^{n-2k-q+z+s,p+y-s}_{l_2m}\,B^{p+y-s}_{m}\,\Xi_{p+q+w+y} \tag{A4}$$

The integrals $A^{q,p}_{lm}$ and B^{p}_{m} are defined and evaluated in Appendix B, and the binomial coefficient $\binom{m}{n} = \frac{m!}{n!(m-n)!}$. Note that because of the factor Ξ_{n+w+z}, only even or odd values of n are needed in the evaluation of $S^{w,y,z}_{n,k}$ which simplifies the sums tremendously. Similarly, the factor $\Xi_{p+q+w+y}$ simplifies the sums over p and q. All dependence on (l_1l_2m) are in the functions $A^{q,p}_{lm}$ and B^{p}_{m}.

Appendix B. Integrals

The integrals B^{p}_{m} are defined as

$$B^{p}_{m} = \frac{1}{2\pi}\int_0^{2\pi}\cos^{p}\phi\,\cos m\phi\,\mathrm{d}\phi \tag{B1}$$

For the case $m=0$, we have

$$B^{p}_{0} = \frac{(p-1)!!}{p!!}\Xi_p = \frac{1}{2^{p-1}}\binom{p-1}{p/2}\Xi_p \tag{B2}$$

where $\Xi_p = 1$ if p is even and 0 if p is odd. $B^{0}_{0} = 1$ and !! means the double factorial (i.e., $n!! = n(n-2)(n-4)\ldots$). For $m>0$, we have

$$B^{p}_{m} = \frac{m}{2}\sum_{k=0}^{\left[\frac{m}{2}\right]}(-1)^{k}2^{m-2k}\frac{(m-k-1)!}{k!(m-2k)!}B_0^{p+m-2k}\Xi_{p+m} \tag{B3}$$

where $[m/2] = m/2$ for m even and $(m-1)/2$ for m odd. Note that $B^{p}_{m} = 0$ if $p = 0$ and $m > 0$.

The integrals $A^{q,p}_{lm}$ are defined as

$$A^{q,p}_{lm} = \frac{1}{2}\int_0^{\pi}\cos^{q}\theta\,\sin^{p+1}\theta\,P_{lm}(\cos\theta)\,\mathrm{d}\theta \tag{B4}$$

Using a series representation for $P_{lm}(x)$,[18] we have

$$A_{lm}^{q,p} = \sum_{k=0}^{\left[\frac{l-m}{2}\right]} (-1)^k \times \left(\frac{(2(l-k))!}{2^{l+1}k!(l-k)!(l-2k-m)!}\right) \times \left(\frac{\Gamma\left(\frac{p+m+2}{2}\right)\Gamma\left(\frac{q+l-2k-m+1}{2}\right)}{\Gamma\left(\frac{p+q+l-2k+3}{2}\right)}\right) \Xi_{q+l+m} \quad \text{(B5)}$$

where $\Gamma(x)$ is the gamma function, $[m/2] = m/2$ for m even and $(m-1)/2$ for m odd, and $\Xi_p = 1$ if p is even and 0 if p is odd.

Appendix C. $\langle P \rangle$

The average pressure in a system of rigid linear molecules whose interactions are described by the site−site potential in eq 5 is given by[19]

$$\langle P \rangle = \rho k_B T - \frac{1}{3V}\left\langle \sum_{i=1}^{2}\sum_{j=1}^{2} \frac{1}{r_{ij}}\frac{\partial v}{\partial r_{ij}}(\boldsymbol{r}_{ij}\cdot\boldsymbol{R}) \right\rangle = \rho k_B T - \frac{2\pi\rho^2}{3}\sum_{l_1 l_2 m}\int g_{l_1 l_2 m}(R) Q_{l_1 l_2 m}(R) R^2 \, dR \quad \text{(C1)}$$

where

$$Q \equiv \sum_{i=1}^{2}\sum_{j=1}^{2} \frac{1}{r_{ij}}\frac{\partial v}{\partial r_{ij}}(\boldsymbol{r}_{ij}\cdot\boldsymbol{R}) \quad \text{(C2)}$$

and $Q_{l_1 l_2 m}(R)$ is the average of Q over the spherical harmonics.

We proceed as for the energy and find

$$\tilde{Q}_{l_1 l_2 m}(R) \equiv \frac{Q_{l_1 l_2 m}(R)}{4\pi N_{l_1 m} N_{l_2 \bar{m}}} = 4R^2 \sum_{n=1}^{\infty} L^{2n} \sum_{k=0}^{n} R^{2n-2k}[G^{(2n-k)} S_{2n,k}^{0,0,0} + L^2 G^{(2n+1-k)}(S_{2n+1,k}^{0,0,1} + S_{2n+1,k}^{1,0,0})] \quad \text{(C3)}$$

where $G^{(n)} = V^{(n+1)}$, which is defined in eq 7. Note that the dependence of $S_{n,k}^{w,x,y}$ on $(l_1 l_2 m)$ is assumed.

The Q_{000} terms can be derived by using the normal expression for the virial for a spherically symmetric potential, i.e., $Q_{000}(R) = R\partial U_{000}/\partial R$, which yields for $v = 1/R^M$ (with $x = b_e/R$)

$$Q_{000}(R) = -\frac{8}{(M-1)!R^M}\{MJ_0(M,x) + 2J_1(M,x)\} \quad \text{(C4)}$$

where the J_n are defined in eqs 12−14. For $v = \exp[-\alpha R]$ (with $x = \alpha b_e$)

$$Q_{000}(R) = -\frac{8e^{-\alpha R}}{\alpha}\left\{\alpha^2 R K_0(x) - 2\left(\alpha + \frac{1}{R}\right)K_1(x)\right\} \quad \text{(C5)}$$

where the K_n are defined in eqs 17−19.

Appendix D. $\langle F^n \rangle$

If the interaction between two linear, homonuclear molecules is described by the site−site potential in eq 5, the force along the bond of one of the molecules (e.g., a) due to the other molecule is $-(\partial U/\partial b_a)$, where b_a is the separation between sites on molecule a. We assume that the length of the other molecule is fixed at the equilibrium bond length b_e and that we will evaluate the force at $b_a = b_e$. The average generalized force on that molecule is then given simply by

$$\langle F^{(n)} \rangle = 4\pi\rho \sum_{l_1 l_2 m}\int g_{l_1 l_2 m}(R) F_{l_1 l_2 m}^{(n)}(R) R^2 \, dR \quad \text{(D1)}$$

where

$$F^{(n)} = \left(\frac{\partial^n v}{\partial b_a^n}\right)_{b_e} \quad \text{(D2)}$$

and the $F_{l_1 l_2 m}^{(n)}(R)$ are found by averaging over the spherical harmonics as done for $U_{l_1 l_2 m}(R)$. The force along the bond is then $f_{l_1 l_2 m}(R) = F_{l_1 l_2 m}^{(1)}(R)$, and the force constant is $k_{l_1 l_2 m}(R) = F_{l_1 l_2 m}^{(2)}(R)$.

For the force $f_{l_1 l_2 m}(R)$, we have

$$\tilde{f}_{l_1 l_2 m}(R) \equiv \frac{f_{l_1 l_2 m}(R)}{4\pi N_{l_1 m} N_{l_2 \bar{m}}} = 2\sum_{n=1}^{\infty} L^{2n+1} \sum_{k=0}^{n} R^{2n-2k}[G^{(2n-k)}(S_{2n,k}^{0,0,0} + S_{2n,k}^{0,1,0}) + R^2 G^{(2n+1-k)} S_{2n+1,k}^{1,0,0}] \quad \text{(D3)}$$

where $G^{(n)} = V^{(n+1)}$, which is defined in eq 10. Note that the dependence of $S_{n,k}^{w,x,y}$ (defined in Appendix A) on $(l_1 l_2 m)$ is assumed.

For $v = 1/R^M$, we find, using eq 10 for $V^{(n)}$ and with $x = b_e/R$,

$$f_{000}(R) = \frac{8}{(M-2)!R^M b_e} J_1(M,x) \quad \text{(D4)}$$

where J_1 can be evaluated using eqs 12−14.

For an exponential site−site potential, $v = \exp[-\alpha R]$, we have, using the expression for $V^{(n)}$ in eq 15 (with $x = \alpha b_e$),

$$f_{000}(R) = \frac{8e^{-\alpha R}}{\alpha b_e}\left\{\alpha K_1(x) - \frac{2}{R}K_2(x)\right\} \quad \text{(D5)}$$

where K_n is defined in eqs 17−19.

The average force constant due to interactions of a molecule with all other molecules in the fluid fixed at their equilibrium bond length is $\langle k \rangle = \langle F^{(2)} \rangle$. We find

$$\tilde{k}_{l_1 l_2 m}(R) \equiv \frac{k_{l_1 l_2 m}(R)}{4\pi N_{l_1 m} N_{l_2 \bar{m}}} = V^{(1)} + \frac{R^2 V^{(2)}}{3} + \sum_{n=1}^{\infty} L^{2n+2}\{\sum_{k=0}^{n} R^{2n-2k} [R^2 V^{(2n+3-k)} S_{2n+2,k}^{0,0,0} + R^4 V^{(2n+4-k)} S_{2n+2,k}^{2,0,0} + V^{(2n+2-k)}(S_{2n,k}^{0,0,0} + 2S_{2n,k}^{0,1,0} + S_{2n,k}^{0,2,0}) + 2R^2 V^{(2n+3-k)}(S_{2n+1,k}^{1,0,0} + S_{2n+1,k}^{1,1,0})] + V^{(n+2)} S_{2n+2,n+1}^{0,0,0} + R^2 V^{(n+3k)} S_{2n+2,n+1}^{2,0,0}\} \quad \text{(D6)}$$

where we take advantage of the restrictions on n in the definition of $S_{n,k}^{w,x,y}$. $V^{(n)}$ is defined in eq 10.

It is possible to evaluate the (000) term analytically and we find for $\upsilon = 1/R^M$, where $x = b_e/R$,

$$k_{000}(R) = \frac{4}{(M-2)!R^M b_e^2}\{2J_2(M,x) - J_1(M,x) + J'_0(M,x)\} \tag{D7}$$

where J_n is defined above and $J'_0 = J_0 - (m-2)!/2$.

For, $\upsilon = \exp[-\alpha R]$ we have

$$k_{000}(R) = \frac{4e^{-\alpha R}}{\alpha b_e^2}\left\{\alpha K'_0(x) - \left(\alpha + \frac{2}{R}\right)K_1(x) + 2\left(\alpha + \frac{1}{R}\right)K_2(x) - \frac{4}{R}K_3(x)\right\} \tag{D8}$$

where K_n is defined above, $K'_0 = K_0 - 1/2$, and $x = \alpha b_e$.

Appendix E. Vibrational Frequency Shifts

We approximate the shift in intramolecular vibrational frequency with a quadratic mean-field model in the spirit of a number of other models and Monte Carlo studies.[2,10,16] We assume that we have one vibrating molecule in a fluid of molecules fixed at their equilibrium bond lengths. Forces and force constants are approximated as equilibrium averages of the first and second derivatives of the intermolecular potential with respect to the bond length of the vibrating molecule.

Since this model has been described in detail elsewhere,[2] we just outline the appropriate expressions. The basic notion is that we describe the intramolecular potential as an expansion about the equilibrium gas-phase bond length, r_e,

$$V_i = \frac{1}{2}kx^2 + \frac{1}{2}gx^3$$

where $x = (r - r_e)$, r is the bond length, and k and g are the usual quadratic and cubic force constants. Even at the highest pressures and temperatures considered in this paper, the deviation from the gas-phase bond length is small enough that this is a good representation of the potential. The gas-phase vibrational frequency is $\omega_o = \sqrt{k/\mu}$. We then assume the following form to describe the centrifugal contribution, which approximates the rotational−vibrational coupling,[2]

$$V_c = k_B T \ln\left(1 + \frac{x}{r_e}\right) \approx f_c x + \frac{1}{2}k_c x^2$$

where $f_c = -2k_BT/r_e$ and $k_c = 2k_BT/r_e^2$. The contribution from other molecules is assumed to have the form

$$V_x = f_x x + \frac{1}{2}k_x x^2$$

where f_x and k_x are determined using the results from Appendix D.

For each pressure and temperature, the equilibrium bond length is modified as $x_m = (r_m - r_e)$, where r_m is the new bond length and is determined by finding the zero of the force. Using the expressions for the force described above (dropping terms of order x_m^2) we have

$$x_m \approx -\frac{f_c + f_x}{k + k_c + k_x}$$

The new frequency is given by $\omega = \sqrt{k_T/\mu}$, where k_T, the second derivative of the total potential evaluated at the new bond length, is given by

$$k_T \approx k + 3gx_m + k_x + k_c$$

References and Notes

(1) Gray, C. G.; Gubbins, K. E. *Theory of Molecular Fluids*; Clarendon: New York; 1984.

(2) Belak, J.; Etters, R. D.; LeSar, R. *J. Chem. Phys.* **1988**, *89*, 1625.

(3) Hemley, R. J.; Eggert, J. H.; Mao, H. K. *Phys. Rev. B* **1993**, *48*, 5779.

(4) Schmidt, S. C.; Schiferl, D.; Zinn, A. S.; Ragan, D. D.; Moore, D. S. *J. Appl. Phys.* **1991**, *69*, 2793. Schiferl, D.; LeSar, R.; Moore, D. S. In *Simple Molecular Systems at Very High Density*; Plenum: New York, 1989; pp 303−330.

(5) Moore, D. S.; Schmidt, S. C.; Shaw, M. S.; Johnson, J. D. *J. Chem. Phys.* **1991**, *95*, 5603.

(6) Schweizer, K. S.; Chandler, D. *J. Chem. Phys.* **1982**, *76*, 2296.

(7) Zakin, M. R.; Herschbach, D. R. *J. Chem. Phys.* **1986**, *85*, 2376. Zakin, M. R.; Herschbach, D. R. *J. Chem. Phys.* **1988**, *89*, 2380.

(8) Lee, M.-R.; Ben-Amotz, D. *J. Chem. Phys.* **1993**, *99*, 10074.. Ben-Amotz, D.; Herschbach, D. R. *J. Phys. Chem.* **1993**, *97*, 2295.

(9) Devendorf, G. S.; Ben-Amotz, D. *J. Phys. Chem.* **1993**, *97*, 2307.

(10) LeSar, R. *J. Chem. Phys.* **1987**, *86*, 4138. Note that the expressions for the attractive contributions are incorrect (eq 6). The coefficients were inadvertently written in that paper as 1/2 the correct values. Equation 4 in the present paper is the expression. Also, the expansion of the repulsive contributions were incorrect for the higher powers of r_e. Equation 19 gives the correct expressions.

(11) Steele, W. A.; Sandler, S. I. *J. Chem. Phys.* **1974**, *61*, 1315.

(12) Fries, P. H.; Patey, G. N. *J. Chem. Phys.* **1985**, *82*, 429. Fries, P. H.; Patey, G. N. *J. Chem. Phys.* **1986**, *85*, 7307. Perera, A.; Kusalik, P. G.; Patey, G. N. *J. Chem. Phys.* **1987**, *87*, 1295.

(13) Downs, J.; Gubbins, K. E.; Murad, S.; Gray, C. G. *Mol. Phys.* **1979**, *37*, 129.

(14) Allen, M. P.; Tildesley, D. J. *Computer Simulation of Liquids*; Oxford University Press: Oxford, UK, 1987.

(15) Etters, R. D.; Chandrasekharan, V.; Uzan, E.; Kobashi, K. *Phys. Rev. B* **1986**, *33*, 8615.

(16) Belak, J. Ph.D. Thesis, Colorado State University, 1988.

(17) There are numerical problems that arise for $1/R^M$ potentials when n in eq 9 (or in the equivalent expressions for other quantities) becomes greater than about 20. For large n, the terms in the series over k are large and alternating in sign. Thus, care must be taken to calculate each of the quantities in eq 11 as accurately as possible, which is why we have written the integrals and sums in Appendices A and B in terms of binomial coefficients, which can be calculated accurately by taking the exponential of the appropriate differences of the logarithms of the factorials and rounding to the nearest integer.

(18) Arfken, G. *Mathematical Methods for Physicists*; Academic Press: 663, 1985. Equation 12.64 in this reference gives a series representation of the Legendre function P_l. An equivalent expression for the associated Lengendre function P_{lm} is found by using the definition $P_{lm}(x) = (1-x^2)^{1/2} d^m/dx^m\, P_l(x)$.

(19) Klein, M. L. In *Molecular Dynamics of Statistical-Mechanical Systems*; North-Holland: New York, 424, 1986.